

Facile synthesis of graphene quantum dots based on electrochemical method and their application for specific Fe³⁺ detection

Yang Fu^{1,2}, Runze Liu¹, Jinfang Zhi^{1, 2*}

¹Key Laboratory of Photochemical Conversion and Optoelectronic Materials, Technical Institute of Physics and Chemistry, Chinese Academy of Sciences, No.29 Zhongguancun East Road, Haidian District, Beijing 100190, PR China

²University of Chinese Academy of Sciences, No.19 Yuquan Road, Shijingshan District, Beijing 100049, PR China

*Corresponding author

DOI: 10.5185/amlett.2018.2052

www.vbripress.com/aml

Abstract

A novel electrochemical strategy for economical, environmental-friendly, simple and facile synthesis of glycine functionalized graphene quantum dots (GQDs) based on direct exfoliation and oxidation from graphite rods was reported. The average diameter of as-synthesized GQDs is 30 nm. Due to the rich nitrogen and oxygen functional groups on the surface of GQDs, the GQDs dispersion was bright yellow and further applied in selective detection of ferric ion (Fe³⁺). A sensor based on photoluminescence quenching of GQDs after adding Fe³⁺ has a limit of detection of 3.09 μM, which is lower than the maximum level (0.3 mg/L, equivalent to 5.4 μM) of Fe³⁺ permitted in drinking water by the U.S. Environmental Protection Agency (EPA). The fluorescent sensor has a wide linear range of 10–150 μM. Moreover, due to the low cytotoxicity of as-prepared GQDs, this study may provide a new analytical platform for further applications of GQDs in real environmental and biological system. Copyright© 2018 VBRI Press.

Keywords: Graphene quantum dots, ferric ion, electrochemical method, fluorescence.

Introduction

Graphene is a two-dimensional monolayer of sp² bonded carbon atoms, it has attracted tremendous attention in energy and sensing applications due to its high conductive network and vast specific surface area [1]. On the other hand, for the zero-band semiconductor material, its hydrophobicity and biotoxicity has hindered their application in biomedicine and optical sensing. Recently, it is reported that curving 2D graphene into 0D graphene quantum dot (GQD) can transform this zero-band semiconductor material into a semiconductor with a wide bandgap due to quantum confinement and edge effects, which indicate a promising application in nanoelectronics [2]. According to the previous reports, GQD has been successfully synthesized and the quantum confinement influenced by the edge and defect effects renders GQDs unique and tunable photoluminescence properties. Therefore, GQDs may have great potentials for bio-imaging [3], optical sensing [4], photovoltaics [5], and so forth.

Recently, many fluorescent materials including organic dyes, metal nanoclusters, conjugated polymers and semiconductor quantum dots (QDs) have been developed for the detection of metal ions. These materials have several advantages compared with conventional techniques, such as fast detection, high sensitivity, and being non-sample destructing [6,7].

However, these reported fluorescent materials as a probe all exhibit intrinsic defects such as heavy metals toxicity, complex synthesis routes, environmental pollution and high-cost, which restricts their applications. Therefore, the development of alternatives with eco-friendliness and low-cost is highly demanded. Graphene quantum dots (GQDs), as a new class of carbon nanomaterials and universal fluorescent material, have received much attention due to their unique and excellent properties, including low toxicity, photostability, high biocompatibility, good water solubility, stable photoluminescence, tunable surface functionalities and easy preparation [8–11]. It may provide an alternative way for metal ions detection.

There are already a few reported methods for metal ions detection using GQDs [12,13]. However, these methods usually showed less advantage on serving as the fluorescence probe to the other conventional materials in terms of sensitivity. This may attribute to the fact that the GQDs do not have satisfactory fluorescence activity, leading to the low detection performance. In addition, the lack of functionality on GQD surfaces may also results in the poor sensitivity during the detection [14]. Therefore, the development of specially functionalized GQDs is essential for applications of GQDs as a new platform in analysis systems.

In this work, we reported a new electrochemical strategy for facile synthesis of specially functionalized GQDs based on a directly electrochemical exfoliation and oxidation of graphite rods in NaOH and glycine. The obtained GQDs are employed for specific and quantitative detection of iron ions (Fe^{3+}) by fluorescence method. The results demonstrate a bright future for GQDs in sensing application.

Experimental

Chemicals and apparatus

High purity graphite rods (\varnothing 6mm, 99.99%) were purchased from Beijing Jinglongtetan Technology Co., Ltd. NaOH and glycine were purchased from Beijing Chemical Reagent. Quinine sulfate (99%, suitable for fluorescence) were supplied by Aladdin. Dialysis bags with a molecular-weight cutoff of about 3 kDa was supplied by Spectrum Labs, USA. All other reagents were of analytical grade and used as received. The solutions of metal ions (Ca^{2+} , Fe^{3+} , Na^+ , K^+ , Ni^{2+} , Co^{2+} , Ag^+ , Mg^{2+} , Zn^{2+} , Cd^{2+} and Al^{3+}) were prepared with ultrapure water from the respective metal salts ($\text{Ca}(\text{NO}_3)_2$, $\text{Fe}(\text{NO}_3)_3$, NaNO_3 , KNO_3 , $\text{Ni}(\text{NO}_3)_2$, $\text{Co}(\text{NO}_3)_2$, AgNO_3 , $\text{Mg}(\text{NO}_3)_2$, $\text{Zn}(\text{NO}_3)_2$, $\text{Cd}(\text{NO}_3)_2$, $\text{Al}(\text{NO}_3)_3$). Ultrapure water used throughout all experiments was purified with the Millipore system.

The IR spectra were recorded on a Fourier-transform infrared spectrometer (EXCALIBUR 3100). The XPS spectra measurements were performed on an X-ray photoelectron spectroscopy (EDAX, GENESIS 60S). The morphology and structure of the samples were investigated by Transmission electron microscopy (TEM, JEM 2100). Atomic Force Microscopy (AFM) images were taken with Scanning Probe Microscope (Bruker Multimode 8, Germany). The absorption spectra of the samples were measured on a UVIKONXL UV-vis spectrophotometer (SECOMAM, France). Fluorescence spectra were obtained by an F-380 fluorescence spectrophotometer with the excitation wavelength of 335 nm. The fluorescence imaging was observed under a laser confocal fluorescence microscope with a 20x objective lens (N-C2-SIM). Electrochemically exfoliated experiments were performed with DC power supply (ITECH Electronic Co., Ltd, USA).

Synthesis of GQDs

The GQDs were synthesized by electrochemical exfoliation of graphite rods in a two-electrode cell configuration, in which the rods were adopted as electrodes (both anode and cathode) and the carbon source. A schematic illustration of the experimental setup is shown in **Fig. 1**. In a typical experiment, two identical graphite rods (10 cm in length and 0.6 cm in diameter) were vertically inserted into the electrolyte at a distance of 1cm, with a working bias voltage of 10V. The electrolyte was prepared by mixing NaOH (0.1M) and glycine (0.067M) in water (200mL). The bias voltage was provided by a DC power supply. The

experiment was conducted under ambient condition for 4 h. As the time proceeded, the electrolyte changed from a colorless solution to yellow and then to dark brown due to corrosion of the graphite anode. The bulky graphitic fragments were separated by centrifugation at 2000 rpm. The as-prepared GQDs exhibit great colloidal stability in water, without leaving any sedimentation even after centrifugation at 10000 rpm. The solid was obtained by rotary evaporation. For further separation and purification, the solid was dissolved in ethanol because GQDs are soluble in water and ethanol but inorganic salt are insoluble in ethanol. The insoluble precipitate in the solution was removed by centrifugation at 10000 rpm. The solution was further purified through dialysis bags ($M_w = 3000$) against distilled water for 1 days. Eventually, pure GQDs were obtained by rotary evaporation. The resulting nanoparticle powder was re-dispersed in ultrapure water for further studies.

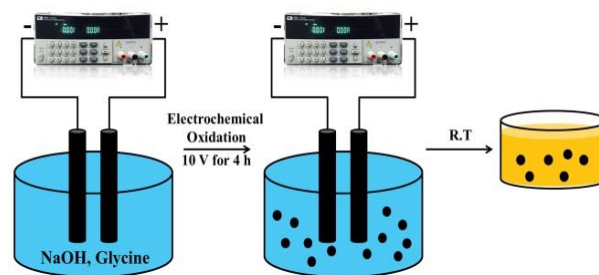


Fig. 1. Schematic illustration for GQDs preparation via electrochemical oxidation of graphite rods.

Detection of ferric ion

The detection of Fe^{3+} ions was performed at room temperature. GQDs were dissolved in ultrapure water to form a 1 mg/mL aqueous solution. 500 μL GQDs solution were added to 10 mL volumetric flasks and then ferric ion (Fe^{3+}) solution ranging from 0 to 400 μM were added at a constant volume with ultrapure water. Fluorescence measurements were carried out with excitation and emission slit width of 10 nm and excitation wavelength was 335 nm. The calibration curve of Fe^{3+} was determined by measuring the change in relative fluorescence intensity at various Fe^{3+} concentrations ranging from 10 to 150 μM .

Results and discussion

Characterization of GQDs

The surface morphology and particle size distribution of as-prepared GQDs were first characterized using TEM and AFM measurements. TEM images revealed quasi-spherical nanoparticles (Figure 2b) with an average particle size about 30 nm. As shown in **Fig. 2a**, the AFM image also shows the uniform distribution of GQDs and the height profiles of the nanoparticles are between 1 and 3 nm, which indicates that the particles are GQDs rather than carbon dots [15].

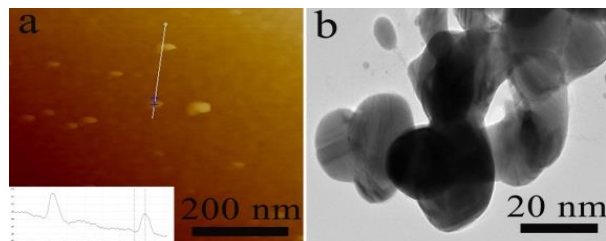


Fig. 2. The characterization of GQDs. (a) AFM image and (b) TEM image.

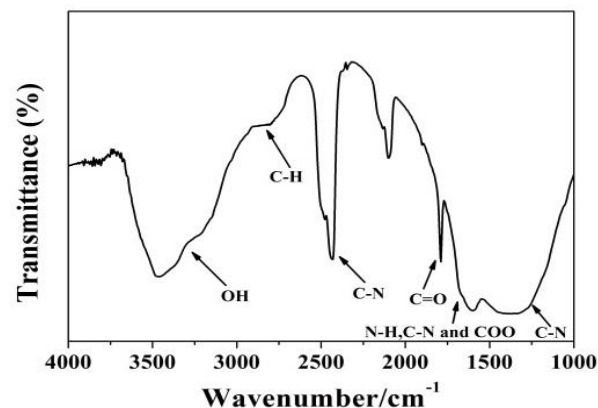


Fig. 3. The FTIR spectra of GQDs.

In order to understand the fundamental structural integrity of the surface functional groups formed in the GQDs, FTIR spectroscopy was analyzed in Fig. 3. The O-H stretching vibrations in the region of 2800–3440 cm^{-1} indicate the presence of hydroxyl groups, which may contribute to the excellent hydrophilic nature of GQDs [16-19]. The strong band observed at 2340 cm^{-1} was assigned to C-N bond. Two sharp bands at 1760 and 1579 cm^{-1} are ascribed to the C=O of the carbonyl groups and the vibrations of N-H, C-N, COO respectively [20,21]. The existence of this band suggested a successful surface passivation reaction of GQDs. The other band related to the C-N stretching vibrations is also shown in 1350 cm^{-1} [22,23].

Moreover, the surface groups were also investigated by XPS analysis. As shown in Fig. 4a, XPS spectra of GQDs confirm the presence of C, O and N with three dominant peaks centered at 531.5 (O 1s), 399.5 (N 1s), and 288.1 eV (C 1s), respectively. The atomic abundance of C, O, N is 73.42 %, 20.43 % and 6.15 %. As shown in Fig. 4b, the C 1s peaks could be deconvoluted into four peaks centered at 285, 286.2 and 288.5, which were assigned to C-C/C=C, C-N/C-O and C=O/CN species, accordingly. The presence of C-C/C=C and C-N/C-O indicate the existence of graphitic structures and interaction with O and N atoms. The deconvoluted peaks of N 1s spectrum in Fig. 4c show pyrrolic N (C-N-C) and N-H contributions at 399 and 401.5 eV [24,25]. The strong pyrrolic contribution in N 1s peak means that the N atoms with ternary structure are situated higher than its primary environment (N-H), which is the evidence on the successful N doping onto the graphitic surface [26]. In addition, the two peaks at 531.0 and 532.0 eV in O 1s spectrum (Fig. 4d) are attributed to C=O and C-OH/C-O-C groups,

respectively. Thus, the results of FTIR and XPS studies gave a good correlation of the presence of these functional groups, which leads to the excellent water solubility of GQDs.

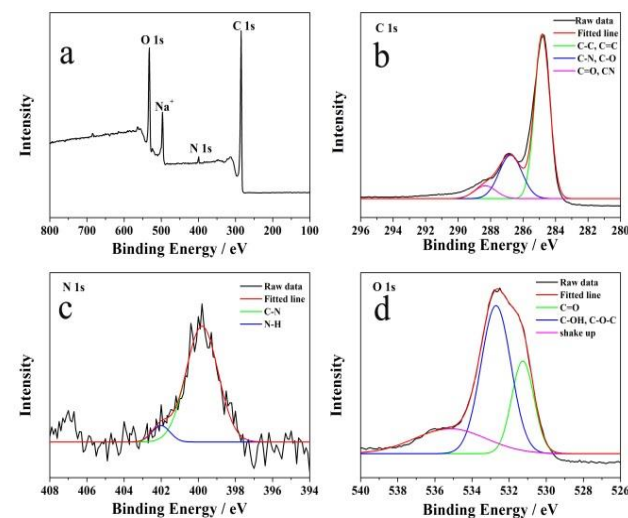


Fig. 4. The XPS spectra of as-prepared GQDs. (a) survey spectra and deconvoluted, (b) C 1s, (c) N 1s and (d) O 1s peaks.

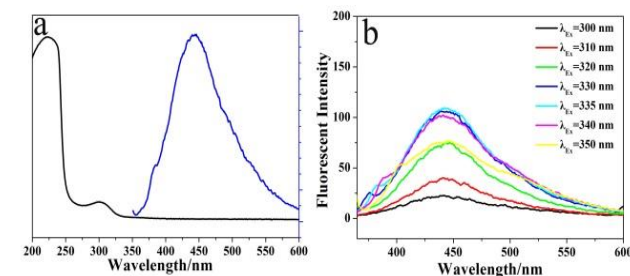


Fig. 5. (a) UV-vis spectrum (black line) and fluorescence spectrum (blue line) of the GQDs aqueous solution. (b) Fluorescence spectra (excitation wavelength from 300 to 350 nm) of GQDs dispersions.

Optical properties

The optical properties of the GQDs were explored through UV/Vis and fluorescence spectroscopy. Fig. 5a depicts the UV/Vis absorption spectrum of the as-synthesized GQDs dispersed in water. The UV excitation spectrum exhibits two peaks (at 250 nm and 335 nm) corresponding to Π - Π^* and n - Π^* transitions. The fluorescence spectra of the aqueous dispersion of GQDs for different excitation wavelengths are reported in Fig. 5b. The PL spectrum collected at $\lambda_{\text{ex}} = 335$ nm exhibits a band at $\lambda = 445$ nm. The band at $\lambda = 445$ nm remains in the same spectral position, even when the excitation wavelength is varied from $\lambda = 300$ nm to 350 nm, which indicate an excitation-wavelength-independent emission. The PL intensity first increases with excitation wavelength and reaches a maximum at $\lambda_{\text{ex}} = 335$ nm and then decreases. As the most direct and important index, the quantum yield (Φ) of GQDs was calculated according to equation (1):

$$\Phi = \Phi_R \times (I/I_R) \times (A_R/A) \times (\eta/\eta_R) \quad (1)$$

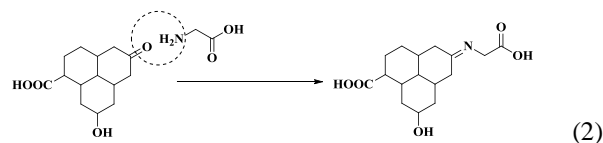
where I is the measured integrated emission intensity, η is the refractive index of the solvent, A is

the optical density, and the subscript R refers to the reference standard with a known Φ (quinine sulfate, $\Phi = 54\%$).

The quantum yield of the GQDs calculated for excitation at $\lambda_{\text{ex}} = 335$ nm by using quinine sulfate as a standard is about 12.65%. The emission is broad for all excitation wavelengths, covering a significant fraction of the visible range.

Possible formation mechanism

According to physico-chemical characterization and previous reports, the exfoliation mechanism can be explained as follows [27, 28, 15]. The electrolyte used was a mixed aqueous solutions of NaOH (0.1 M) and glycine (0.067 M) in water (200 mL). The aqueous solution of NaOH contains Na^+ and OH^- ions. By applying a potential about 10 V, which is higher than the electrochemical potential of water (1.23 V), water is dissociated into H^+ and OH^- ions. Upon further anodic oxidation, hydroxyl and oxygen radicals may be generated. These radicals could attack the graphite surface from edge states/grain boundaries and promote intercalation [28]. Due to electrochemical oxidation, hydroxyl, carbonyl and carboxyl functional groups are also attached to the surface of the nanoparticles. In the last step, glycine undergoes a condensation reaction with the carbonyl group and is functionalized on GQDs [15]. The resultant functional groups on GQDs can be presented as shown in Equation (2):



Application

In addition to the distinct optical properties, the obtained GQDs also exhibited good stability. Even after being kept for two weeks at room temperature, the photo-luminescence intensity keeps strong. Furthermore, the cell viabilities of HeLa cells were tested after being exposed to GQDs at a series of concentrations and the as-obtained results indicate that GQDs exhibited low cytotoxicity to HeLa cells (Fig. S1). Therefore, the GQDs possess good potential as nanoparticles in bio-imaging and optical sensing. Subsequently, we demonstrated the application of the GQDs in metal ion detection and cell imaging.

Detection of ferric ion (Fe^{3+})

The impacts of different metal ions (all at 200 μM) including Fe^{3+} , Mg^{2+} , Co^{2+} , Ni^{2+} , Ag^+ , Al^{3+} , Cd^{2+} , Cu^{2+} , Pb^{2+} , Ca^{2+} , Na^+ , K^+ on the photoluminescence intensity of the GQDs were studied. The fluorescence intensities of GQDs were significantly decreased in the presence of Fe^{3+} , while the other ions displayed weak or even negligible effects on their fluorescence intensities (Fig. 6). These observations reflect that the fluorescence of GQDs have specific response to Fe^{3+} , and therefore could be used for the assay of Fe^{3+} .

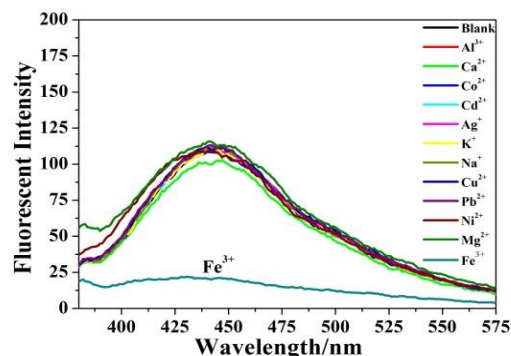


Fig. 6. Photoluminescence emission spectra of solutions of GQDs in the presence of various metal ions. The concentration of GQDs and metal ions were 50 $\mu\text{g}/\text{mL}$ and 200 μM , respectively.

Owing to the unique optical properties, small size, good solubility, photostability, chemical inertness and biocompatibility of as-prepared GQDs, we speculated that glycine functionalized GQDs may be employed to optically detect Fe^{3+} as a new fluorescent sensor. The photoluminescence quenching of GQDs by Fe^{3+} should be ascribed to the specific affinity between Fe^{3+} and the functional groups including oxygen and nitrogen, such as amino, carboxyl or hydroxyl groups on the surface of the GQDs. The interaction between the GQDs and Fe^{3+} resulted in GQDs aggregation, which appears to have caused the photoluminescence quenching of the GQDs [29, 30, 13]. To further prove the feasibility of Fe^{3+} detection, the concentration dependent fluorescence measurements of GQDs at various concentrations of Fe^{3+} were monitored. As shown in Fig. 7a, fluorescence intensity of GQDs was decreased with the addition of various concentrations of Fe^{3+} ranging from 0 to 400 μM , and there was a notable and linear decrease in the fluorescence intensity over a wide concentration range of Fe^{3+} (from 10 to 150 μM) (Fig. 7b). The detection limit was calculated to be 3.09 μM ($= 3\sigma/S$ where σ is the standard deviation, S is the slope of the linear response), which is lower than the maximum level (0.3 mg/L, equivalent to 5.4 μM) of Fe^{3+} permitted in drinking water by the U.S. Environmental Protection Agency (EPA) [31]. Moreover, the results of this method are compared with those previously reported fluorescent methods for Fe^{3+} detection, which are listed in Table 1. It can be seen that as-prepared GQDs is more sensitive than those previous reports for detection of Fe^{3+} , which further demonstrate the potential applications of this novel sensor in determination of Fe^{3+} .

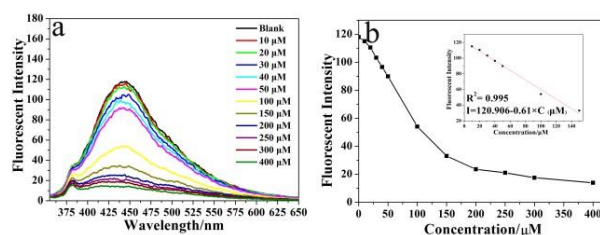


Fig. 7. (a) Photoluminescence emission spectra of GQDs in the presence of various concentrations of Fe^{3+} ranging from 0 to 400 μM , (b) the correlation curve between the fluorescent intensity and the concentration of Fe^{3+} (calibration linear curve).

Table 1. Comparison of the LOD for the detection of Fe³⁺.

Methods	Linear range (μM)	LOD (μM)	Ref
GQDs	0-80	7.22	[12]
DOPA-mediated fluorescent gold nanoclusters	5-1280	3.5	[32]
2,6-Bis(2-Benzimidazolyl) Pyridine Fluorescent Red-Shifted Sensor	–	3.5	[33]
GQDs	10-150	3.09	This work

Conclusion

Herein, as-synthesized GQDs were facilely produced by the electrochemical method with an average diameter of 30 nm. Meanwhile, based on characterization and comparison results, it can be concluded that GQDs exhibit non-shifting fluorescence emissions at 445 nm due to the oxidation of surface states to make quantum confinement and edge effects. In addition, the as-prepared GQDs were used for specific and sensitive detection of Fe³⁺ with broad linear ranges of 10–150 μM as well as present a low limit of detection of 3.09 μM. Furthermore, characteristics of low cytotoxicity were demonstrated, which confirmed that the GQDs can be used as promising candidates for chemical analysis and biological applications.

Acknowledgements

This work was supported by the Beijing Graphene Science and Technology Innovation Project (Grant No.Z161100002116026) .

Author's contributions

Conceived the plan: YF, JZ; Performed the experiments: YF, JZ; Data analysis: YF; Wrote the paper: YF, JZ. Authors have no competing financial interests.

Supporting information

Supporting informations are available from VBRI Press.

References

- Liu, Y.; Dong, X.; Chen, P; Chem. Soc. Rev., **2012**, 41, 2283. DOI: [10.1039/C1CS15270J](https://doi.org/10.1039/C1CS15270J)
- Li, Y.; Hu, Y.; Zhao, Y.; Shi, G.Q.; Deng, L.E.; Hou, Y.B.; Qu, L.T; Adv. Mater., **2011**, 23, 776. DOI: [10.1063/1.4928028](https://doi.org/10.1063/1.4928028)
- Dong, Y.Q.; Chen, C.Q.; Zheng, X.T.; Gao, L.L.; Cui, Z.M.; Yang, H.B.; Guo, C.X.; Chi, Y.W.; Li, C.M; J. Mater. Chem., **2012**, 22, 8764. DOI: [10.1039/C2JM30658A](https://doi.org/10.1039/C2JM30658A)
- Li, Y.H.; Zhang, L.; Huang, J.; Liang, R.P.; Qiu, J.D; Chem. Commun., **2013**, 49, 5180. DOI: [10.1039/C3CC40652K](https://doi.org/10.1039/C3CC40652K)
- Gupta, V.; Chaudhary, N.; Srivastava, R.; Sharma, G.D.; Bhardwaj, R.; Chand, S; J. Am. Chem. Soc., **2011**, 133, 9960. DOI: [10.1021/ja2036749](https://doi.org/10.1021/ja2036749)
- Koneswaran, M.; Narayanaswamy, R; Sens. Actuators B, **2009**, 139, 91–96. DOI: [10.1016/j.snb.2008.09.011](https://doi.org/10.1016/j.snb.2008.09.011)
- Chen, Y.; Rosenzweig, Z; Anal. Chem., **2002**, 74, 5132–5138. DOI: [10.1021/ac0258251](https://doi.org/10.1021/ac0258251)
- Baker, S.N.; Baker, G.A; Angew. Chem. Int. Ed., **2010**, 49, 6726–6744. DOI: [10.1002/anie.200906623](https://doi.org/10.1002/anie.200906623)
- Kwon, W.; Lee, G.; Do, S.; Joo, T.; Rhee, S.W; Small, **2014**, 10, 506–513. DOI: [10.1002/smll.201301770](https://doi.org/10.1002/smll.201301770)
- Zhang, S.; Wang, Q.; Tian, G.; Ge, H; Mater. Lett., **2014**, 115, 233–236. DOI: [10.1016/j.matlet.2013.10.086](https://doi.org/10.1016/j.matlet.2013.10.086)
- Jiang, F.; Chen, D.; Li, R.; Wang, Y.; Zhang, G.; Li, S.; Zheng, J. Huang, N.; Gu, Y.; Wang, C; Nanoscale, **2013**, 5, 1137–1142. DOI: [10.1039/C2NR33191H](https://doi.org/10.1039/C2NR33191H)
- Ananthanarayanan, A.; Wang, X.W.; Routh, P.; Sana, B.; Lim, S.; Kim, D.H.; Lim, K.H.; Li, J.; Chen, P; Adv. Funct. Mater., **2014**, 24, 3021–3026. DOI: [10.1002/adfm.201303441](https://doi.org/10.1002/adfm.201303441)
- Liu, M.L.; Xu, Y.H.; Niu, F.S.; Justin Gooding, J.; Liu, J.Q; Analyst, **2016**, 141, 2657–2664. DOI: [10.1039/C5AN02231B](https://doi.org/10.1039/C5AN02231B)
- Chowdhury, A.D.; Doong, R.A; ACS Appl. Mater. Interfaces, **2016**, 8, 21002–21010. DOI: [10.1021/acsami.6b06266](https://doi.org/10.1021/acsami.6b06266)
- Joseph, J.; Anappara, A.A; ChemPhysChem, **2017**, 18, 292–298. DOI: [10.1002/cphc.201601020](https://doi.org/10.1002/cphc.201601020)
- Cui, X.; Wang, Y.; Liu, J.; Yang, Q.; Zhang, B.; Gao, Y.; Sens. Actuators B: Chem., **2017**, 242, 1272–1280. DOI: [10.1016/j.snb.2016.09.032](https://doi.org/10.1016/j.snb.2016.09.032)
- Chen, Y.; Wu, Y.; Weng, B.; Wang, B.; Li, C; Actuators B: Chem., **2016**, 223, 689–696. DOI: [10.1016/j.snb.2015.09.081](https://doi.org/10.1016/j.snb.2015.09.081)
- Jiang, J.; He, Y.; Li, S.; Cui, H; Chem. Commun., **2012**, 48, 9634–9636. DOI: [10.1039/C2CC34612E](https://doi.org/10.1039/C2CC34612E)
- Qu, D.; Zheng, M.; Du, P.; Zhou, Y.; Zhang, L.; Li, D; Nanoscale, **2013**, 5, 12272–12277. DOI: [10.1039/C3NR04402E](https://doi.org/10.1039/C3NR04402E)
- Zheng, Y.; Yang, D.; Wu, X.; Yan, H.; Zhao, Y.; Feng, B; RSC Adv., **2015**, 5, 90245–90254. DOI: [10.1039/C5RA14720D](https://doi.org/10.1039/C5RA14720D)
- Zhu, C.; Zhai, J.; Dong, S; Chem. Commun., **2012**, 48, 9367–9369. DOI: [10.1039/C2CC33844K](https://doi.org/10.1039/C2CC33844K)
- Zhang, J.; Yang, L.; Yuan, Y.; Jiang, J.; Yu, S.H; Chem. Mater., **2016**, 28, 4367–4374. DOI: [10.1021/acs.chemmater.6b01360](https://doi.org/10.1021/acs.chemmater.6b01360)
- Peng, H.; Travas-Sejdic, J; Chem. Mater., **2009**, 21, 5563–5565. DOI: [10.1021/cm901593y](https://doi.org/10.1021/cm901593y)
- Qu, D.; Zheng, M.; Zhang, L.; Zhao, H.; Xie, Z.; Jing, X; Sci. Rep., **2014**, 4, 5294. DOI: [10.1038/srep05294](https://doi.org/10.1038/srep05294)
- Doong, R.A.; Liao, C.Y.; J. Hazard. Mater., **2017**, 322, 254–262. DOI: [10.1016/j.jhazmat.2016.02.065](https://doi.org/10.1016/j.jhazmat.2016.02.065)
- Anh, N.T.N.; Chowdhury, A.D.; Doong, R; Sens. Actuators B: Chem., **2017**, 252, 1169–1178. DOI: [10.1016/j.snb.2017.07.177](https://doi.org/10.1016/j.snb.2017.07.177)
- Rao, K.S.; Senthilnathan, J.; Liu, Y.F.; Yoshimura, M; Sci. Rep., **2014**, 4, 4237. DOI: [10.1038/srep04237](https://doi.org/10.1038/srep04237)
- Li, X.; Zhao, Z; RSC Adv., **2014**, 4, 57615–57619. DOI: [10.1039/C4RA09274K](https://doi.org/10.1039/C4RA09274K)
- Zhang, S.; Li, J.; Zeng, M.; Xu, J.; Wang, X.; Hu, W; Nanoscale, **2014**, 6, 4157–4162. DOI: [10.1039/C3NR06744K](https://doi.org/10.1039/C3NR06744K)
- Li, Z.X.; Zhang, L.F.; Zhao, W.Y.; Li, X.Y.; Guo, Y.K.; Yu, M.M.; Liu, J.X; Inorg. Chem. Commun., **2011**, 14, 1656–1658. DOI: [10.1016/j.inoche.2011.06.032](https://doi.org/10.1016/j.inoche.2011.06.032)
- Wu, H.L.; Yang, L.; Chen, L.F.; Xiang, F.; Gao, H.Y; Anal. Methods, **2017**, 9, 5935–5942. DOI: [10.1039/c7ay01917c](https://doi.org/10.1039/c7ay01917c)
- Annie Ho, J.; Chang, H.C.; Su, W.T; Anal. Chem., **2012**, 84, 3246–3253. DOI: [10.1021/ac203362g](https://doi.org/10.1021/ac203362g)
- Razavi, B.V.; Badieli, A.; Lashgari, N.; Ziarani, G.M; J Fluoresc., **2016**, 26, 1723–1728. DOI: [10.1007/s10895-016-1863-7](https://doi.org/10.1007/s10895-016-1863-7)